[CONTRIBUTION FROM THE EASTERN REGIONAL RESEARCH LABORATORY[1]]

Structure of Alkali Amylose

BY F. R. SENTI AND L. P. WITNAUER

X-Ray diffraction studies of the structure of amylose and amylose complexes have been limited for the most part to preparations which give powder patterns. Less ambiguous interpretations of structure can be given fiber patterns, but oriented preparations are required, which are difficult to prepare by conventional methods owing to the low wet strength and hydrophilic character of amylose films.

These difficulties can be circumvented by orienting a non-hydrophilic derivative of amylose and then converting this derivative to amylose under such conditions that orientation is retained. Amylose triacetate serves this purpose well, for it is easily oriented by stretching in glycerol at 170°. Oriented alkali amylose is produced directly on deacetylation of clamped filaments in alcoholic alkali solution. Alkali amylose can be converted to the A, B[2] and V structural modifications by methods previously described.[3]

All structural modifications give well-defined fiber patterns. The alkali amyloses give patterns especially rich in reflections and, because they constitute an isomorphous series, their patterns can be more readily interpreted than those of the other modifications.

Experimental

Amylose was prepared by twice fractionating autoclaved potato starch with nitrobenzene.[4] Acetylation was carried out by the method of Whistler, Jeanes and Hilbert,[5] and films about 0.25 mm. thick were cast from chloroform solution. Strips 2 to 4 mm. wide were oriented by stretching in glycerol[6] at 170°. Films stretched 500% are highly oriented, as evidenced by their diffraction pattern, and are suitable for deacetylation.

In the deacetylation experiments, 3- to 10-centimeter filaments of oriented amylose triacetate were held taut in stainless steel clamps and suspended in the various deacetylating solutions. Unless clamped, the filaments retract considerably, especially at higher alkali concentrations, and give disoriented diffraction diagrams. The characteristic diffraction pattern of potassium hydroxide amylose is given by filaments deacetylated at 25° in 0.01 to 0.30 *N* potassium hydroxide (carbonate-free) in 75% ethanol. Completion of deacetylation has been checked by analysis of the filaments and is also evidenced by the disappearance of the amylose triacetate reflections from the diffraction pattern.

That ethanol is not an integral part of the structure is demonstrated by the identical patterns produced by filaments deacetylated in 0.25 *N* potassium hydroxide in 75% ethanol, 75% methanol, saturated butanol or in water. Deesterification proceeds slowly in the last two media and is accompanied by breakage of many filaments in the aqueous alkali solutions.

Filaments from which the alkali has been removed by extraction with absolute methanol give amorphous diffraction diagrams. Extraction with 75% methanol or ethanol results in fiber patterns characteristic of the "V structure. Reconstitution, by soaking in 0.2 *N* potassium hydroxide in 75% ethanol, restores the original diffraction pattern.

Amylose triacetate filaments deacetylated in 75% ethanol, 0.01 to 0.30 *N* in lithium or cesium hydroxide, give the characteristic diffraction patterns of lithium hydroxide amylose and cesium hydroxide amylose. At the higher concentration of alkali (above 0.3 *N* potassium hydroxide, for example) the characteristic fiber pattern diminishes in intensity and is gradually replaced by a diffuse pattern of the V-type.

Sodium hydroxide and guanidine in 75% ethanol likewise deacetylate amylose triacetate and produce the corresponding alkali amyloses with characteristic X-ray diagrams. No systematic study of the composition of these filaments or those of ammonium hydroxide amylose, prepared as described below, has been made. The similarity of their diffraction patterns to those of lithium, potassium, and cesium hydroxide amylose, however, indicates that they have the same structure and composition as the latter.

Preparation of an alkali amylose is not limited to the deacetylation of amylose triacetate by the corresponding hydroxide, but is also accomplished by the exchange of one alkali for another. For example, cesium hydroxide amylose results when potassium hydroxide amylose is immersed in alcoholic cesium hydroxide. Thallium hydroxide amylose has been obtained in similar manner. Barium hydroxide can be exchanged for potassium hydroxide, but the resulting fiber gives a poorly defined diffraction pattern. Attempts to prepare ammonium hydroxide amylose by deacetylation have failed, whereas exchange with alcoholic ammonia solutions has been successful.

(1) One of the Laboratories of the Bureau of Agricultural and Industrial Chemistry, Agricultural Research Administration, United States Department of Agriculture. Article not copyrighted.

(2) Fiber patterns of the B structural modification have been described by R. E. Rundle, L. Daasch and D. French, THIS JOURNAL, **66**, 130 (1944).

(3) F. R. Senti and L. P. Witnauer, *ibid.*, **68**, 2407 (1946).

(4) R. L. Whistler and G. E. Hilbert, *ibid.*, **67**, 1161 (1945).

(5) R. L. Whistler, H. Jeanes and G. E. Hilbert, *ibid.*, in press (1948).

(6) Method of N. C. Schieltz, private communication.

Many salts in aqueous alcohol solution can be exchanged for the alkali in alkali amylose. By this method we have obtained compounds of amylose with the iodide, bromide, acetate, formate and propionate of potassium. All give excellent fiber diffraction patterns, which will be described in another publication.

Alkali and Water Content.—On removal from the deacetylating solution, the clamped filaments were wiped dry with absorbent tissue to remove adhering alkali solution. Adsorbed alcohol, which is difficult to remove by vacuum drying, was removed by humidification of the filaments over water in a vacuum desiccator for sixteen to twenty-four hours. The vacuum-dried filaments were weighed, excess acid added, and titrated with sodium hydroxide. Figure 1 presents data on the alkali content of the filaments as a function of the normality of the deacetylation solution.

It is to be noted that the alkali content of the filaments increases rapidly with concentration of base in the deacetylation solution up to a normality of 0.02. Above 0.02 *N*, the alkali content of the fibers increases at a much lower rate, and the composition curve is nearly horizontal over a range of normalities, particularly in the case of cesium and potassium hydroxide. At higher normalities, the slope of the composition curve again increases. These observations suggest stoichiometric compound formation between amylose and alkali at a composition corresponding to the horizontal portion of the curve. For cesium hydroxide amylose, this composition corresponds to an alkali content of 26%, whereas for potassium and lithium hydroxide amyloses, the alkali contents are 11 and 5%, respectively. The observed values are in satisfactory agreement with those calculated from the formula $1MOH \cdot 3C_6H_{10}O_5$, which requires 23.7% cesium hydroxide, 10.3% potassium hydroxide and 4.7% lithium hydroxide.

At both extremes of the composition curve, however, the alkali content of the filaments deviates considerably from that corresponding to the stoichiometric ratio $1MOH:3C_6H_{10}O_5$, and the problem of the distribution of the alkali arises. One possibility is that the alkali is distributed at random among a number of crystallographically related sites, which are progressively filled as the alkali content increases. On this hypothesis we should expect the relative intensities of the diffraction maxima to vary with the alkali content. Since the lithium, potassium and cesium amyloses appear to be isomorphous, the magnitude of the shift in relative intensities is indicated by a comparison of the patterns of cesium and potassium amylose having the same mole per cent. alkali. On the cesium amylose ($1CsOH:3C_6H_{10}O_5$) pattern, $I_{(101)} \ll I_{(200)}$, whereas for potassium amylose ($1\ KOH:3C_6H_{10}O_5$), $I_{(101)} \gg I_{(200)}$. If the amount of potassium is increased and the cesium is decreased until the two isomorphous structures con-

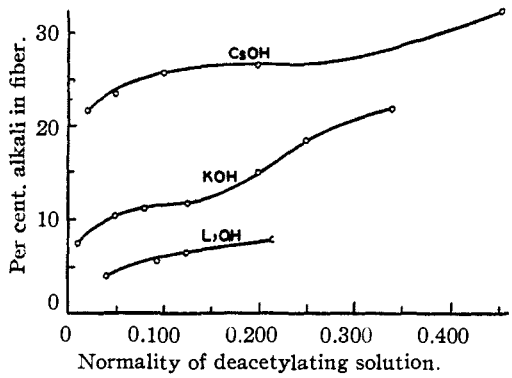

Fig. 1.—Alkali content of lithium, potassium and cesium hydroxide amylose as a function of the normality of alkali in the deacetylating solution.

tain equivalent alkali on the basis of scattering power, the ratio $I_{(101)}/I_{(200)}$ should be the same for the two patterns. Since the scattering factor of cesium is three times that for potassium, patterns of cesium amylose of composition approximately $0.5CsOH:3C_5H_{10}O_5$ were compared with those of potassium amylose of composition approximately $1.5KOH:3C_6H_{10}O_5$. For each pattern, the ratio $I_{(101)}/I_{(200)}$ was unchanged within the error of visual estimation, and it is certain that the inequalities indicated above were not reversed. Random substitution in a set of sites related by symmetry is thus not consistent with our observations.

It appears more likely that the crystalline portions of the fibers are essentially constant in composition with respect to the symmetry-related alkali. Alkali present in other sites would not affect the relative intensities of the discrete diffraction maxima but would contribute to the amorphous background. Any large excess would be expected to distort the structure, causing a change in lattice constants and resulting ultimately in a new or amorphous structure. The possibility that the amorphous regions of the filaments increase in extent and contain an excess or deficiency of alkali at the extremes of composition is not excluded. Experimentally, it is observed that the background scattering increases and the discrete maxima diminish in intensity when the filaments have either a low or high alkali content.

The water content of lithium, potassium and cesium hydroxide amyloses was determined at several humidities after preliminary humidification at 85% R.H. to remove adsorbed ethanol. Humidities were maintained by saturated salt solutions in vacuum desiccators. Water contents on desorption are given in Table I. Diffraction patterns were taken of filaments enclosed in glass capillaries after equilibration at the humidities listed in Table I. Below 30% R.H., corresponding to a water content of about 10%, the patterns diminished in intensity, and there was a slight decrease in lattice dimensions. Precise values of the lattice dimensions of the dry fibers were not determined because accurate measurement of the

weak patterns was impossible. A water content of 10% corresponds to one molecule of water per glucose residue, and this is concluded to be the normal content in the crystalline regions of the filaments.

TABLE I

MOISTURE CONTENT OF ALKALI AMYLOSE AT 25° IN PER CENT. OF DRY WEIGHT ON DESORPTION

Relative humidity, %	Water, %, in LiOH–Amylose	KOH–Amylose	CsOH–Amylose
50	12.6	12.9	11.4
30	9.7	9.9	9.0
12.5	6.3	6.3	6.0

It should be noted that lithium hydroxide amylose also occurs in a more highly solvated structure. Filaments deacetylated in 0.2 *N* lithium hydroxide in 75% ethanol and X-rayed while moist with deacetylating solution give an X-ray pattern showing the same fiber repeat period (22.6 kX), but at least one lateral identity period larger than that of the normal hydrate to which the structure reverts upon drying in air. Under the conditions of deacetylation we have employed, neither cesium nor potassium hydroxide amylose has given any indication of a more highly solvated structure.

X-Ray Diffraction Patterns.—Patterns for indexing were taken in a cylindrical cassette of 5-cm. radius with filtered CuK_α radiation. Filaments mounted with the fiber axis along the cylinder axis show only the second-order reflection of the fiber repeat period. To observe the higher orders, filaments were oscillated with the fiber axis perpendicular to the cylinder axis. Superposition of reflections from planes not perpendicular to the fiber axis on the desired orders of the fiber repeat period was prevented by restriction of the oscillation range. By maintaining a common reflection on succeeding photographs, it was possible to compare the relative intensities of the various orders. Relative intensities of the meridian (orders of the fiber identity period) reflections of lithium, potassium and cesium amyloses were placed on a common basis by the comparison of timed photographs of filaments of known thickness and alkali content. Intensities were estimated visually by comparison with a scale of known relative intensities.

Unit Cell.—The fiber identity period of the alkali amyloses is readily determined from the layer line separation on cylindrical cassette patterns or from the *d*-values of the various orders of the fiber identity period obtained from the oscillation photographs. Determination of the lateral identity periods is ambiguous. The assumption was made that a reflection corresponding to a primitive lateral translation would appear on at least one of the eight layer lines observed. Thus, the first and second nearest reflections to the meridian were indexed as $0kl$ and $lk0$, respectively, where k is the layer line index. On the further assumption that the lattice is orthorhombic, sin θ values were computed and compared with the observed values. The results for potassium hydroxide amylose, based on the orthorhombic unit having $a_0 = 12.7$ kX, $b_0 = 22.6$ kX, and $c_0 = 9.0$ kX, are presented in Table II. A comparison of the dimensions of the orthorhombic unit cells found for the alkali amyloses is given in Table III. All reflections were indexed on the patterns of lithium and cesium hydroxide, whereas the unit cell dimensions of sodium, ammonium and guanidinium hydroxide amylose were derived from measurement of equatorial reflections and layer line separations alone. The lateral dimensions increase regularly with increasing size of the cation except for cesium hydroxide amylose, which has a smaller a_0 than expected. Since the fiber repeat period remains the same, the decrease in a_0 is probably due to a small rotation of the glucose residues about the *b*-axis, and it is unlikely that this will affect the validity of the isomorphous relations which we apply.

Potassium hydroxide amylose containing 10% potassium hydroxide and 13% water has a density (determined by flotation in carbon tetrachloride–petroleum ether mixtures) of 1.53. If it is assumed that the water and alkali are uniformly distributed throughout the filaments, then the number of glucose residues (mol. wt. 162) in the unit cell is

$$N = \frac{12.7 \times 9.0 \times 22.6 \times 1.53 \times 0.77}{162 \times 1.65} = 11.4$$

A similar computation for cesium hydroxide amylose (28.1% cesium hydroxide, 9.0% water, $d = 1.86$) gives a value of 11.3 for N. Consequently, there are twelve glucose residues in the orthorhombic unit cell.

Space Group.—If the alkali amylose structures are based on an orthorhombic lattice, as appears likely from the agreement of observed and calculated sin θ values, the space group must be isomorphous with the point group D_2. All other point groups of the orthorhombic system contain planes of symmetry which are not permitted by the optically active amylose molecules.

Of the reflections $(0k0)$, only those with k even were observed out to $k = 16$ in lithium, potassium and cesium hydroxide amyloses. It is therefore probable that the structures possess a twofold screw axis parallel to the fiber axis. Observed reflections of the form $(h00)$ and $(00l)$ are consistent in all cases with twofold screw axis in the directions *a* and *c*, although not sufficient orders were observed to establish this beyond a possibility of doubt. The observed reflections thus allow space groups $P_{2_12_12_1}$, $P_{22_12_1}$, $P_{2_122_12}$, and P_{22_12}.

Intensity considerations, however, permit only space group $P_{2_12_12_1}$. This follows from the Patterson projections $P_v(uw)$ of the lithium (Fig. 2) and potassium hydroxide (Fig. 3) amyloses. Since the amylose chains lie along *b* (fiber axis), the projection $P_v(uw)$ should give lateral vector distances *u*,

TABLE II

COMPARISON OF CALCULATED AND OBSERVED SIN θ VALUES FOR POTASSIUM HYDROXIDE AMYLOSE

hkl	Sin θ (obs.)	Sin θ (calcd.)	*I* (est.)	*hkl*	Sin θ (obs.)	Sin θ (calcd.)	*I* (est.)
101	0.1049	0.1049	S^+	130	0.1188	0.1183	W^-
200	.1207	.1210	W^-	131	.1457	.1461	W^-
201	.1488	.1483	W	230	.1571	.1580	M
002	.1708	.1714	S^-	231	.1806	.1797	W
202	.2107	.2098	W^-	330	.2071	.2080	M
302	.2495	.2496	M	132		.2082	
401	.2563	.2567	W^+	331	.2246	.2249	M
003		.2571		133	.2831	.2830	W^+
203	.2843	.2841	W	233	.3009	.3018	W^-
501	.3150	.3143	W^+	432	.3148	.3134	W diff.
303		.3147		531	.3303	.3304	W diff.
600	.3637	.3629	W^-	532	.3613	.3622	W diff.
204		.3635		234	.3780	.3774	W diff.
602	.4005	.4014	W^-				
305	.4653	.4653	W^-	140	.1483	.1484	S^-
703	.4954	.4953	W^-	041	.1608	.1603	M
				141	.1719	.1714	W^-
111	.1097	.1102	S^+	240	.1825	.1817	W^-
210	.1254	.1256	S^+	241	.2016	.2009	M^-
211	.1533	.1521	W^-	042	.2179	.2185	W^+
012	.1754	.1747	M	142	.2273	.2267	M^+
310	.1845	.1846	M^+	340		.2265	
112		.1849		341	.2427	.2421	W
311	.2034	.2035	M	043	.2905	.2906	W^+
212	.2118	.2125	M^-	441		.2902	
411	.2585	.2589	W^+	244	.3888	.3879	W^-
013		.2593		640		.3874	
113	.2665	.2663	W	642	.4230	.4236	W^-
213	.2862	.2861	W				
412	.3025	.2984	W	150	.1797	.1799	W^- diff.
510		.3043		051	.1901	.1898	M
313	.3160	.3165	W	151	.1993	.1992	W^-
511		.3162		250	.2091	.2082	W^-
512	.3506	.3493	W^-	251	.2254	.2251	M^-
214	.3652	.3651	W^-	350	.2486	.2482	W^-
610		.3645		152		.2484	
513	.4000	.3984	W^-	351	.2629	.2626	W
612		.4028		153	.3136	.3138	W
414	.4213	.4209	W^-	253	.3314	.3308	W^+
115	.4337	.4340	W^-	353	.3573	.3574	W^-
711		.4333		551		.3571	
120	.0905	.0908	W	160	.2129	.2121	W^-
121	.1253	.1249	S^+	161	.2287	.2287	M
220	.1391	.1387	W^+	261	.2535	.2516	M
221	.1634	.1630	W^-	162	.2718	.2727	M diff.
122	.1945	.1940	S	360		.2725	
320		.1937		262	.2918	.2921	M diff.
321	.2113	.2118	W^-	460	.3162	.3160	W^+
222	.2200	.2205	W^-	163	.3335	.3333	W^+
420	.2512	.2513	W	462	.3593	.3595	W
421	.2672	.2655	W				
023		.2659					
520	.3084	.3099	W				
124	.3574	.3546	M diff.				
423		.3593					
523	.4023	.4027	W^+ diff.				

w between the chains. Resolution of individual carbon and oxygen atoms cannot be expected, since there will be much overlapping in the projection, and furthermore, early termination of the

TABLE III

UNIT CELL DIMENSIONS OF ALKALI AMYLOSES

Amylose	a_0, kX	b_0 (fiber axis), kX	c_0, kX
LiOH	12.1	22.6	8.8
NaOH	12.3	22.6	8.9
KOH	12.7	22.6	9.0
NH_4OH	12.7	22.6	9.0
CsOH	12.4	22.6	8.9
$C(NH_2)_3OH$	13.1	22.6	9.0

series required by the observed reflections results in low inherent resolution. We interpret the maxima in Figs. 2 and 3 at (0, 0) and ($^1/_2$, $^1/_2$) to indicate two amylose chains in the unit cell separated by the vector distance ($^1/_2$, $^1/_2$). Such an

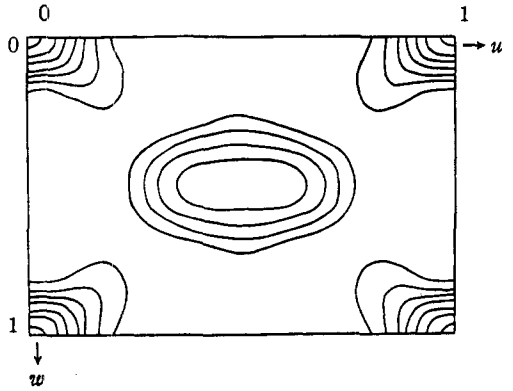

Fig. 2.—Patterson function $P_v(uw)$ for lithium hydroxide amylose.

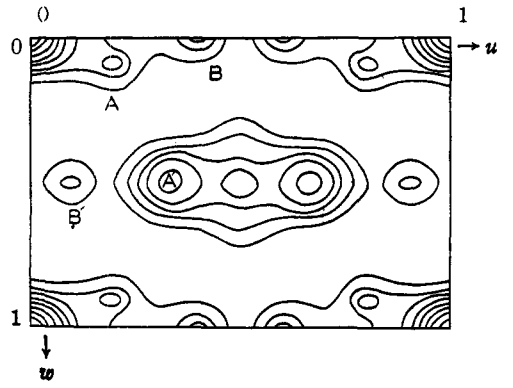

Fig. 3.—Patterson function $P_v(uw)$ for potassium hydroxide amylose.

arrangement is consistent with space group $P_{2_12_12_1}$ as indicated in Fig. 4, where the chains lie on the screw axis along b. Since the amylose molecule does not possess twofold symmetry, it cannot lie on a twofold axis, and a structure based on $P_{2_22_12}$ would have four chains in the orthorhombic cell. Disposition of the four chains in the unit cell according to symmetry requirements and packing considerations demands a Patterson projection having maxima at approximately ($^1/_2$, 0) and (0, $^1/_2$) in addition to the observed maximum at ($^1/_2$, $^1/_2$). Likewise, structures based on $P_{2_12_12}$ or $P_{2_22_12_1}$ can be eliminated by comparison of their projected intermolecular vectors with the observed Patterson projection.

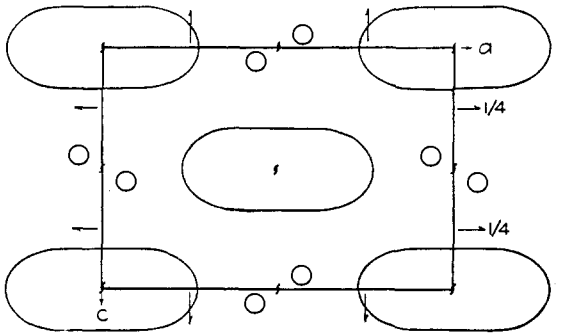

Fig. 4.—Projection of the alkali amylose structure on (010), showing position of amylose chains and alkali ions.

Isomorphism of the Alkali Amyloses.—The near identity of the unit cell dimensions and the fact that all diffraction patterns are consistent with space group $P_{2_12_12_1}$, indicate that the alkali amyloses are isomorphous. Further evidence is provided by a comparison of the $|F|$-values (Table IV) of the ($0k0$) reflections of lithium, potassium and cesium hydroxide amyloses. Filaments having the same content of alkali on a mole basis (1 mole alkali/3 glucose units) were used for this purpose. Appropriate corrections were made for the time of exposure, sample thickness, absorption, Lorentz and polarization factors. The assumption was made that all filaments are equally crystalline. This appears reasonable, since all filaments were prepared from amylose triacetate stretched and deacetylated under identical conditions except for the variation of the alkali. If the structures are isomorphous then

$$\frac{|F|_{0k0}\text{ (KOH-Amylose)} - |F|_{0k0}\text{ (LiOH-Amylose}}{|F|_{0k0}\text{ (CsOH-Amylose)} - |F|_{0k0}\text{ (KOH-Amylose)}} = \frac{f_{K^+} - f_{Li^+}}{f_{Cs^+} - f_{K^+}}$$

where the f's represent the ionic scattering factors. At low angles the value of the ratio is $^1/_2$ and decreases with increasing angles. Thus $|F|_{0k0}$(KOH-Amylose) − $|F|_{0k0}$(LiOH-Amylose) = $^1/_2$ to $^1/_3[|F|_{0k0}$(CsOH-Amylose) − $|F|_{0k0}$(KOH-Amylose)] for the orders considered. These differ-

TABLE IV

F-VALUES FOR THE ($0k0$) REFLECTIONS OF LITHIUM, CESIUM AND POTASSIUM HYDROXIDE AMYLOSES

$0k0$	(1) F_{LiOH}- Amylose	(2) $\|F\|_{KOH}$- Amylose	(3) $\|F\|_{CsOH}$- Amylose	(4) (2)−(1)	(5) (3)−(2)	(6) (3)−(2) Calcd.
020	1	6	22	5	16	−14.7
040	(−) 7	10	18	3	8	− 7.8
060	0	11	35	11	24	+24.0
080	(+) 17	9	9	8	18	−20.4
0·10·0	0	0	0	0	0	0
0·12·0	(−) 25	12	8	13	20	+20.4
0·14·0	<1	4	15	4	11	−19.8
0·16·0	(−) 10	5	17	5	22	+ 7.8

ences are listed in Table IV,[7] in columns 4 and 5, respectively. The agreement is satisfactory, considering the difficulty of making accurate intensity measurements.

Structure of the Alkali Amyloses.—The lateral arrangement of the amylose chains and alkali ions in the isomorphous structures is evident from the Patterson projections of Figs. 2 and 3. Owing to its low scattering, lithium ion contributes little to the Patterson projection, and the maxima in Fig. 2 result from glucose–glucose interactions. Elongation of the maxima in Fig. 2 indicates that the planes of the glucose residues are nearly parallel to the *ab* plane, as represented in Fig. 4. Since there are twelve glucose residues in the unit cell, each of the positions indicated in Fig. 4 must correspond to the projection of six glucose residues. Alkali ion parameters are determined by comparison of Figs. 2 and 3; the additional maxima in the latter result from potassium-potassium and potassium-amylose interactions. Assigning maxima A and A' to the former and maxima B and B' to the latter, the structure represented in Fig. 4 is derived with alkali ions at approximately $x = \frac{24}{60} a_0$, $z = \frac{3}{60} c_0$ and positions derived by symmetry.

Patterson projections of the structure perpendicular to b (the fiber axis) should give the y parameter of the glucose residues and the alkali ions. Unfortunately, the superposition of reflections of different forms having nearly identical $\sin\theta$ values does not permit the assignment of F^2-values to the forms which contribute to the functions $P_w(uv)$ and $P_u(vw)$. The Patterson projections $P_{uw}(v)$ on the fiber axis can be evaluated, however, since only forms $(0k0)$ contribute, and the corresponding F^2-values were determined from oscillation photographs. $P_{uw}(v)$ for cesium hydroxide amylose is given in Fig. 5. Because of the high scattering factor of cesium, the dominant peaks in this function should correspond to Cs^+–Cs^+ distances along b. According to Fig. 5, these distances are $^1/_6\ b_0$.

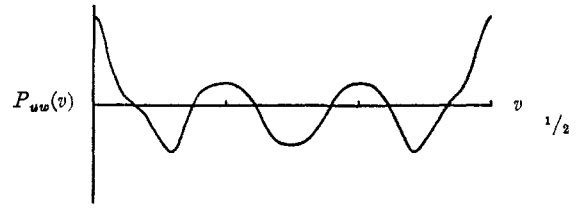

Fig. 5.—Patterson function $P_{uw}(v)$ for cesium hydroxide amylose.

The data of Table IV should also determine the y parameter of the alkali ions, for $|F|_{0k0}$ (Cesium hydroxide–Amylose) $-|F|_{0k0}$ (KOH-Amylose) represents the contribution of an alkali ion of scattering factor $f_{Cs^+} - f_{K^+}$ to the amplitude of the reflection $(0k0)$. Column 6 of Table IV gives the calculated F-values for an alkali ion at $y = 63°$ using a scale factor to give agreement with the observed value for (060). The agreement with the observed values of column 5 are satisfactory except for (0·14·0) and (0·16·0). Part of this discrepancy may be due to error in intensity measurements of the high orders which appeared as weak reflections on the photographs. From the sign of the contribution of the alkali ions to the structure amplitudes of the $(0k0)$ reflections, we can determine the sign of the F-values of lithium hydroxide amylose (as given in column 2 of Table IV). A Fourier series using these values gives the projection of the amylose chain on [010]. This projection appears in Fig. 6 and has maxima at $y = 2/60$, $y = 7.5/60$, $y = 13/60$ and positions related by the center of symmetry of the projection. If it is assumed that these peaks correspond to the centers of the glucose residues of the two amylose chains which have been projected on [010], then we can consider that one chain is displaced with respect to the other by 5.5/60 b_0 or by about one half the projected length (10/60 b_0) of a glucose residue on the fiber axis. This interpretation, however, is somewhat doubtful, because models of extended amylose chains show that there are concentrations of atoms roughly 5/60 b_0 along its axis. The Fourier projection would then be explained by placing the two chains in the unit cell with their centers at the same level along b.

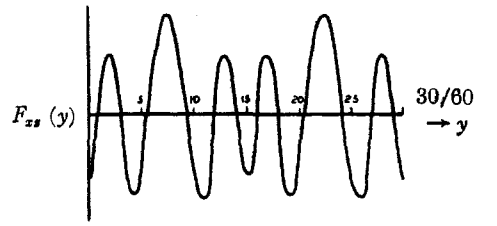

Fig. 6.—Fourier projection of lithium hydroxide amylose on [010].

The exact configuration of the glucose residues in alkali amylose can be determined only by a complete structural analysis, which involves the location of thirty-three atoms of the three independent residues. Fourier series methods have limited application in this case, and the analysis would have to be carried out by trial-and-error methods which we have not attempted. A frequently used but less satisfactory procedure is the comparison of the observed fiber repeat period with that calculated on the basis of various chain configurations.

If it is assumed that all glucose residues have the symmetrical chair configuration[8] with the

(7) The signs of the F_{0k0}'s for lithium hydroxide–amylose which appear in parentheses were determined by the procedure described in the following section.

(8) Pierce, *Trans. Faraday Soc.*, **42**, 545 (1946), has shown that the unit cell dimensions and the intensities of the meridian reflections of cellulose are consistent with the symmetrical chair configuration of the glucose residues. We have used Pierce's bond distances and angles with the exception of the C–C distance, which we take as 1.54 kX instead of 1.52 kX.

bond distances C—C = 1.54 kX, C—O = 1.43 kX and all angles tetrahedral except the ring angle C—O—C, which was taken as 90°, the projection of six maximally extended residues is computed to be 22.4 kX. A chain of maximally extended residues in this configuration does not possess the required twofold screw symmetry, and rotation of the residues to give the required symmetry decreases the fiber repeat period. Bond angles or lengths must be changed, therefore, to obtain agreement with the observed fiber repeat period of 22.6 kX. If the symmetrical chair configuration of minimum steric repulsion is retained, the most reasonable change is to increase the oxygen angle in the ring. Increasing this angle to 109° and using the same values as above for all other angles and distances, the projection of six maximally extended residues is computed to be 26.1 kX. It is evident that models can be constructed having the symmetrical chair configuration and satisfying the requirements of twofold screw symmetry and the observed fiber repeat period by selecting a value for the ring oxygen angle between 90 and 109°. Such agreement, of course, does not eliminate from consideration models of the amylose chain based on other configurations of the glucose ring.

In the structure proposed, the effective thickness of the glucose residue is 4.5 Å., which is consistent with the value found in cellulose and alkali cellulose.[9] The width of the glucose residues plus the contribution of alkali and water (position undetermined) is 12.7 Å., again consistent with the corresponding value found in sodium cellulose III.[8]

Summary

Amylose forms crystalline addition compounds with lithium, sodium, potassium, ammonium, cesium and guanidinium hydroxide. Diffraction patterns indicate these compounds constitute an isomorphous series based on the orthorhombic space group $P_{2_12_12_1}$. Analyses of lithium, potassium and cesium hydroxide amylose shows their composition to be $3C_6H_{10}O_5 \cdot MOH \cdot 3H_2O$, and it is probable that this formula represents the composition of the entire series.

All compounds have the same fiber repeat period, 22.6 kX, corresponding to the extension of six glucose residues. Positions of the alkali ions and the lateral packing of the amylose chains have been determined with the aid of Patterson projections.

(9) K. H. Meyer, L. Misch and N. P. Badenhuizen, *Helv. Chim. Acta*, **22**, 59 (1939).

PHILADELPHIA 18, PA. RECEIVED OCTOBER 20, 1947

[CONTRIBUTION FROM THE DEPARTMENT OF CHEMISTRY, UNIVERSITY OF CHICAGO, AND PHYSICAL CHEMICAL RESEARCH, ENGINEERING DIVISION, CHRYSLER CORPORATION]

Surfaces of Solids. XVIII. The Heats of Emersion and Desorption of Water from Graphite at 25°

BY PAUL R. BASFORD, GEORGE JURA AND WILLIAM D. HARKINS

I. Introduction

A recent paper,[1] gives the adsorption isotherms of water and *n*-heptane on a sample of graphite with a content of less than 0.004% ash and presumably free from oxygen. In that paper some of the problems associated with the graphite–water system were indicated, but their discussion was deferred until after the completion of the calorimetric study of the system as presented here.

II. Experimental

The graphite, furnished through the courtesy of Dr. Lester L. Winter of the National Carbon Company, is described elsewhere. The calorimeter and technique of the measurements was that of Harkins and Jura.[2] Because of the low area of the sample, 4.22 sq. m. g.$^{-1}$, the limited supply of the powder and the small amount of water adsorbed per gram, the technique of Harkins and Jura[2] for determining the amount of water adsorbed could not be used. Instead, the equilibrium pressure of the adsorbed vapor was determined. The amount of adsorbed water was then obtained from the data of the isotherm. For high values of p/p_0 this leads to a considerable uncertainty in the exact amount adsorbed. However the actual results in this region are such that this error is insignificant.

(1) W. D. Harkins, G. Jura and E. H. Loeser, THIS JOURNAL, **68**, 554 (1946).

(2) W. D. Harkins and G. Jura, *ibid.*, **66**, 919 (1944).

III. Experimental Results

The heat of emersion of graphite as a function of the amount of water adsorbed (molecules per sq. cm.) is exhibited in Fig. 1. Each value listed in Table I is the average of either two or three determinations, usually three. The table gives also the number of determinations and the average deviation of each determination. From this table it is possible to calculate all the heat values given.

Unfortunately, the results are not very precise, due to (1) low area coupled with small heat effects per unit area, and (2) difficulty of dispersion. The absolute error in a single determination is about twice that of Harkins and Jura[2] in their cor-